

Supplement.

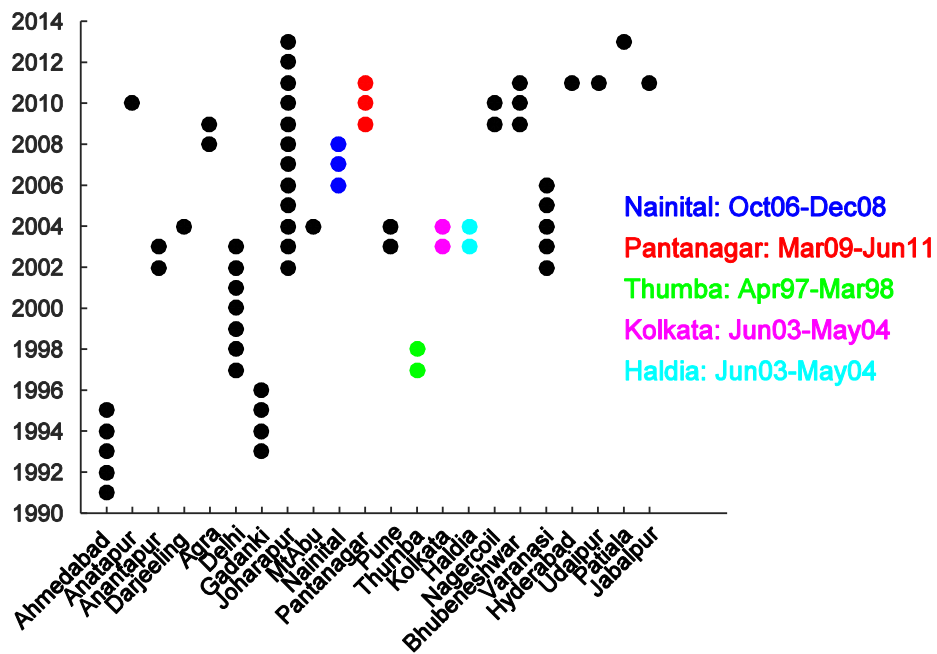


Figure S1. Period of the O₃ measurements for each station in India used in the evaluation. The black dots correspond to the full year and the colored dots represent the partial years. The given period for these partial years with their corresponding station are given in the colored caption.

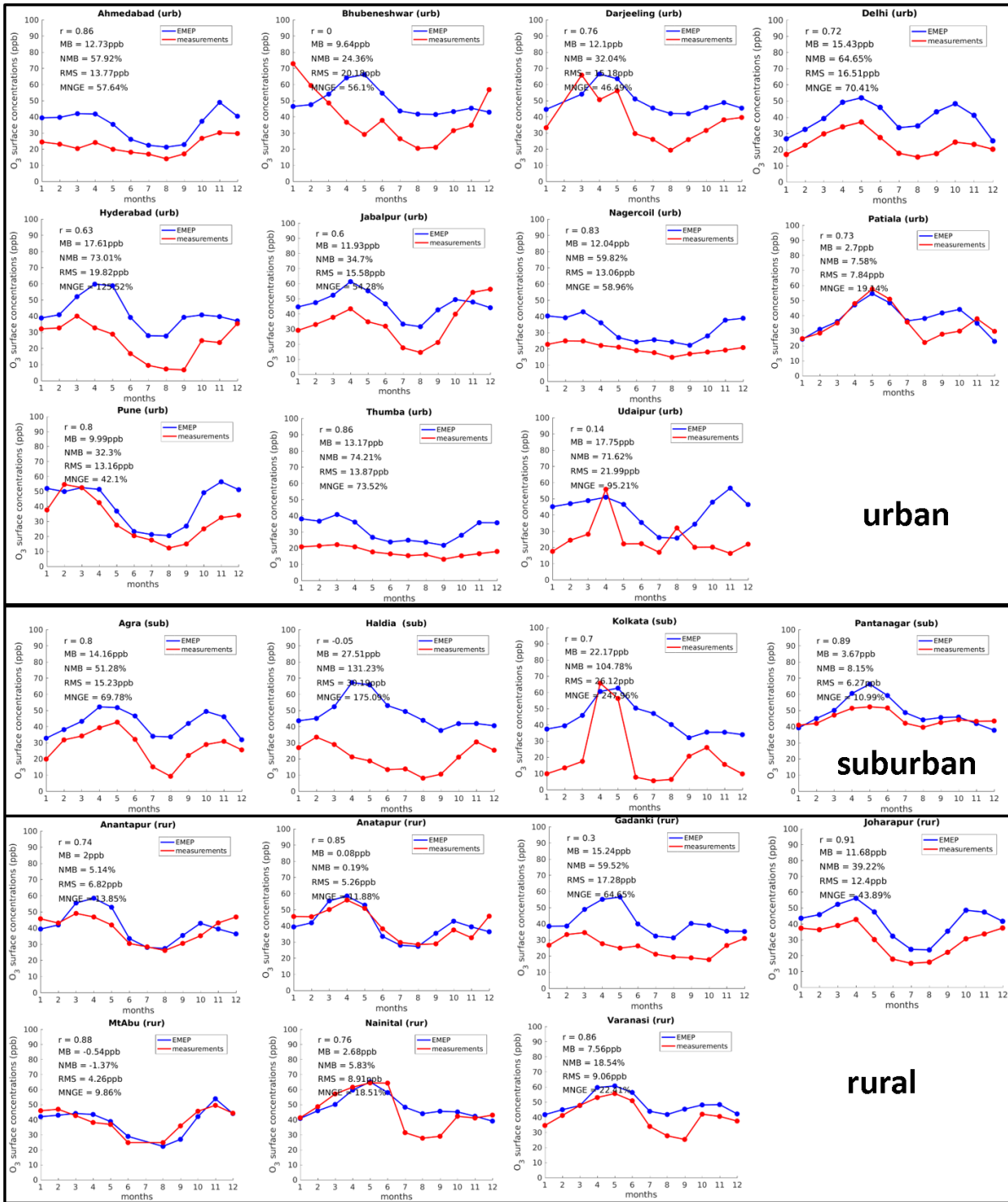


Figure S2. Monthly surface O₃ mean concentrations for all the stations used in Fig. 2. The observations are plotted in red and EMEP (averaged over the period of simulation) in blue. EMEP concentrations are collocated to each station. The correlation coefficient (r), the mean bias (MB), the normalized mean bias (NMB), the Root-Mean-Square (RMS) error, and the mean normalized gross error (MNGE) are provided.

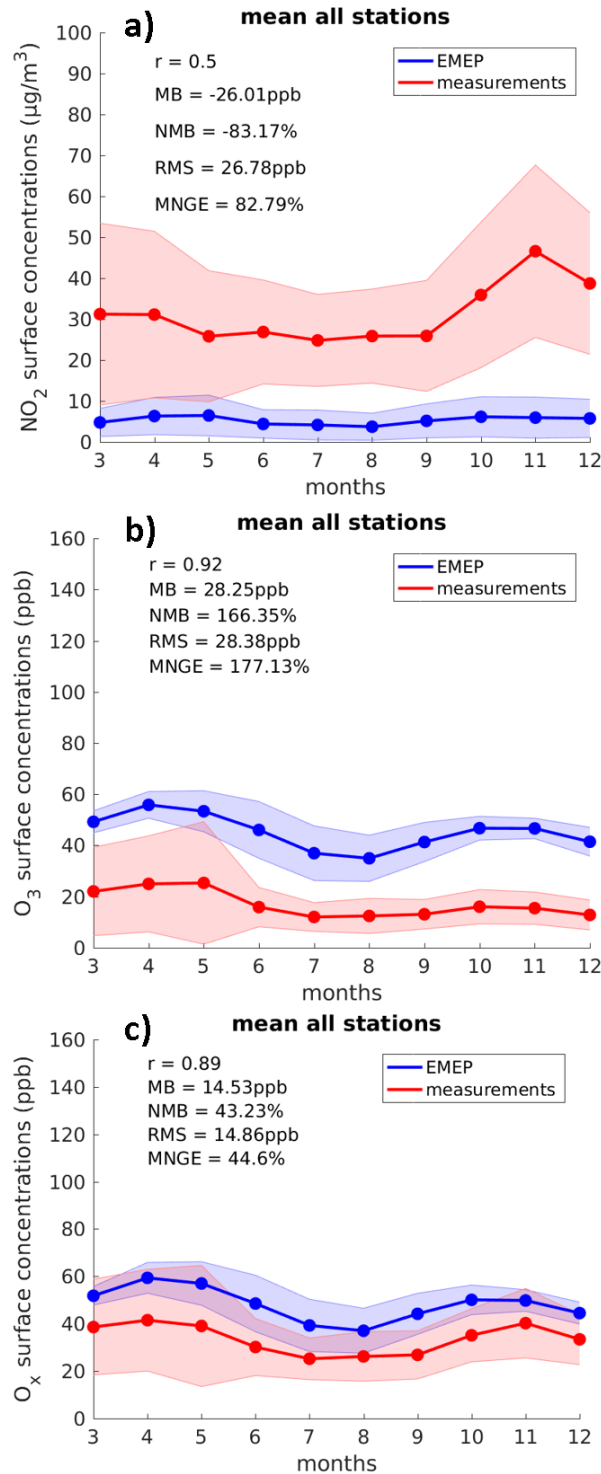


Figure S3. Monthly surface NO₂ (a), O₃ (b) and O_x (c) (O_x = O₃ + NO₂) mean concentrations. The NO₂ and the O₃ concentrations are in $\mu\text{g}/\text{m}^3$, and the O_x (converted from the O₃ and NO₂ concentrations) is in ppb. Each plot shows the measurements from the 14 urban stations measuring continuously from March to December 2016 (red) and the result from EMEP for the reference scenario (averaged over the period of simulation) (blue). EMEP concentrations are collocated to each station. The dataset is from <https://openaq.org>. The shade error corresponds to the standard deviation. The correlation coefficient (r), the mean bias (MB), the normalized mean bias (NMB), the Root-Mean-Square (RMS) error, and the mean normalized gross error (MNGE) are provided. January and February were filtered out due to the limited numbers of stations available (no stations measured NO₂ and O₃ from January to December 2016).

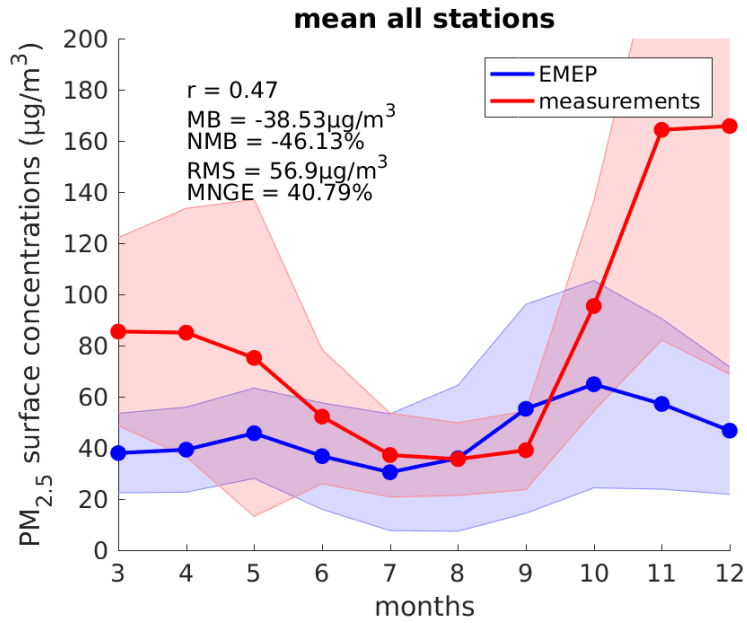


Figure S4. Monthly surface $\text{PM}_{2.5}$ mean concentrations in $\mu\text{g}/\text{m}^3$ for 13 urban stations measuring continuously from March to December 2016 (red) and EMEP for the reference scenario (averaged over the period of simulation) (blue). EMEP concentrations are collocated to each station. The dataset is from <https://openaq.org>. The shade error corresponds to the standard deviation. The correlation coefficient (r), the mean bias (MB), the normalized mean bias (NMB), the Root-Mean-Square (RMS) error, and the mean normalized gross error (MNGE) are provided. January and February were filtered out due to the limited numbers of stations available (only 3 stations measured $\text{PM}_{2.5}$ from January to December 2016).

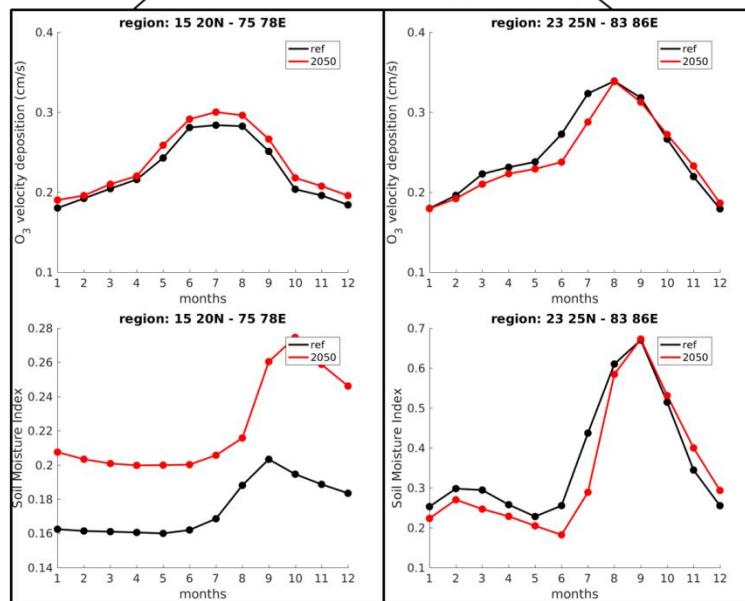
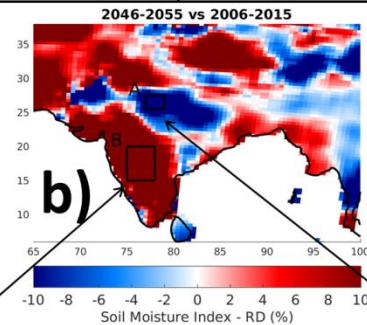
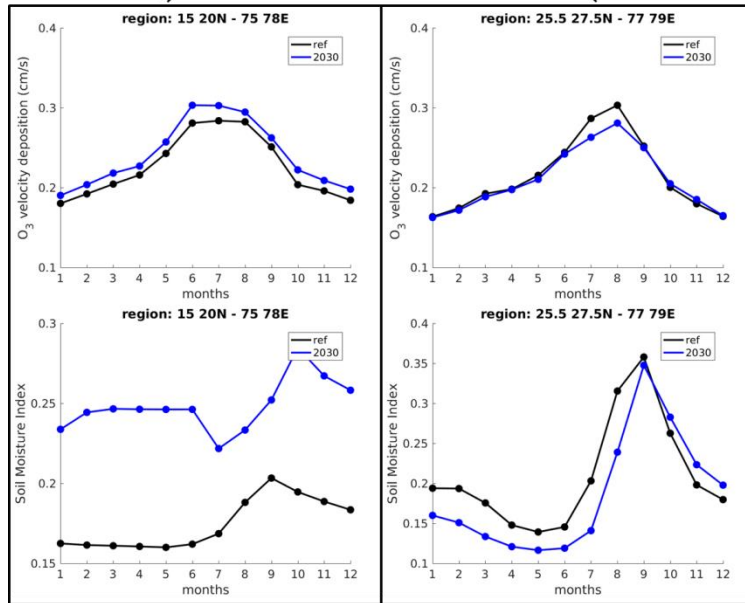
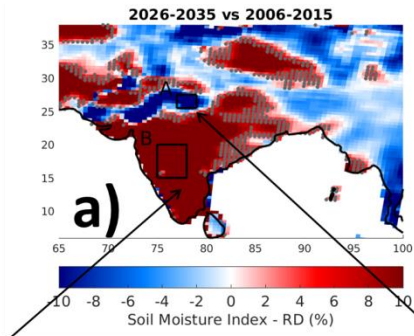


Figure S5. Distribution of the relative difference in soil moisture index between the reference scenario and the FC scenarios (top panel), time-series of the monthly O_3 deposition velocity (middle panels) and time-series of the monthly soil moisture index (bottom panels) for both regions labeled on the maps. The relative difference is calculated as: $([FC - \text{reference}] / \text{reference}) \times 100\%$. The results for the FC2030 scenario are plotted in (a) and for the FC2050 scenario are plotted in (b). The values for the reference scenario are plotted in black and those for the FC2030 scenario in blue and for the FC2050 scenario in red. On the maps, grey dots mark grid points that do not satisfy the 95% level of significance.

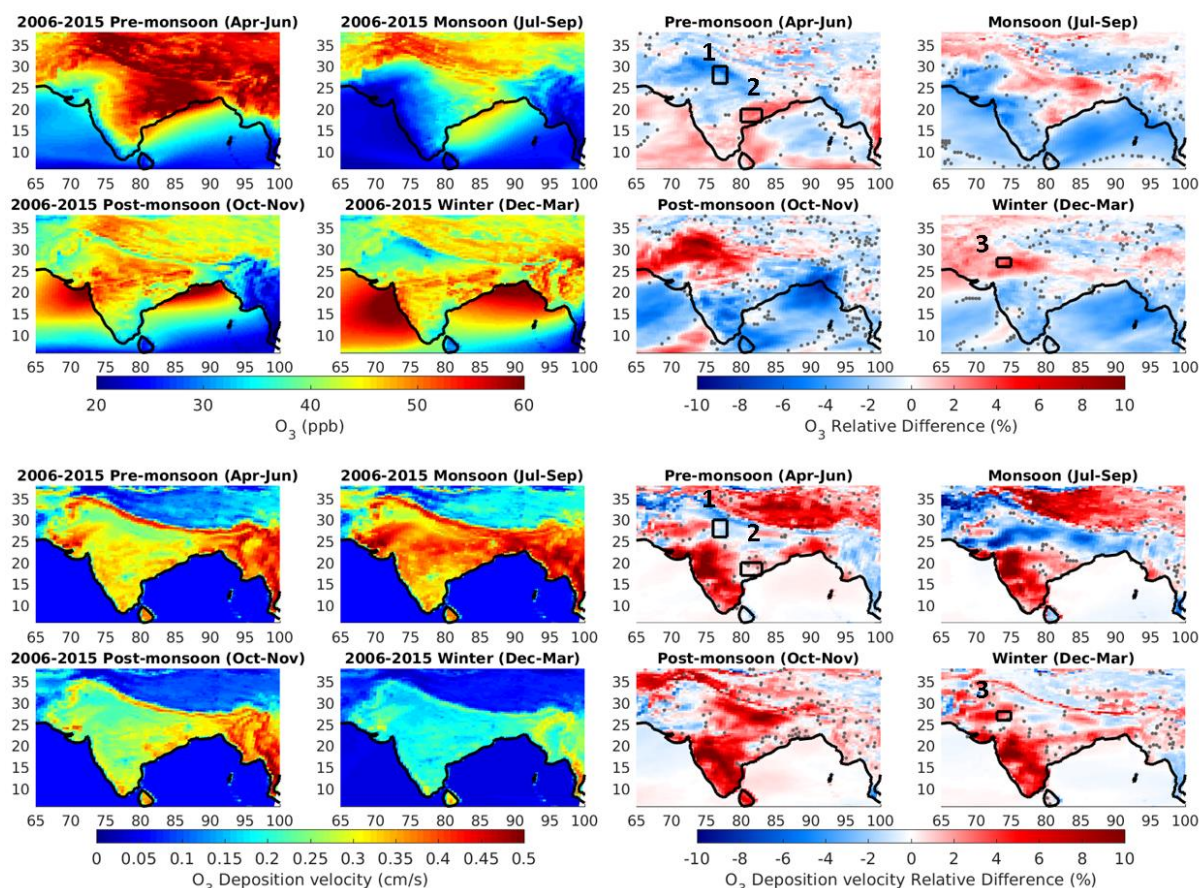


Figure S6. Seasonal distribution of O_3 and relative difference between the reference scenario and the FC2030 scenario (top panels), seasonal distribution of O_3 deposition velocity and relative difference between the reference scenario and the FC2030 scenario (bottom panels). The relative differences are calculated as: $([FC2030 - \text{reference}] / \text{reference}) \times 100\%$. Regions discussed in the text are numbered on the distributions of relative difference. Grey dots mark grid points that do not satisfy the 95% level of significance.

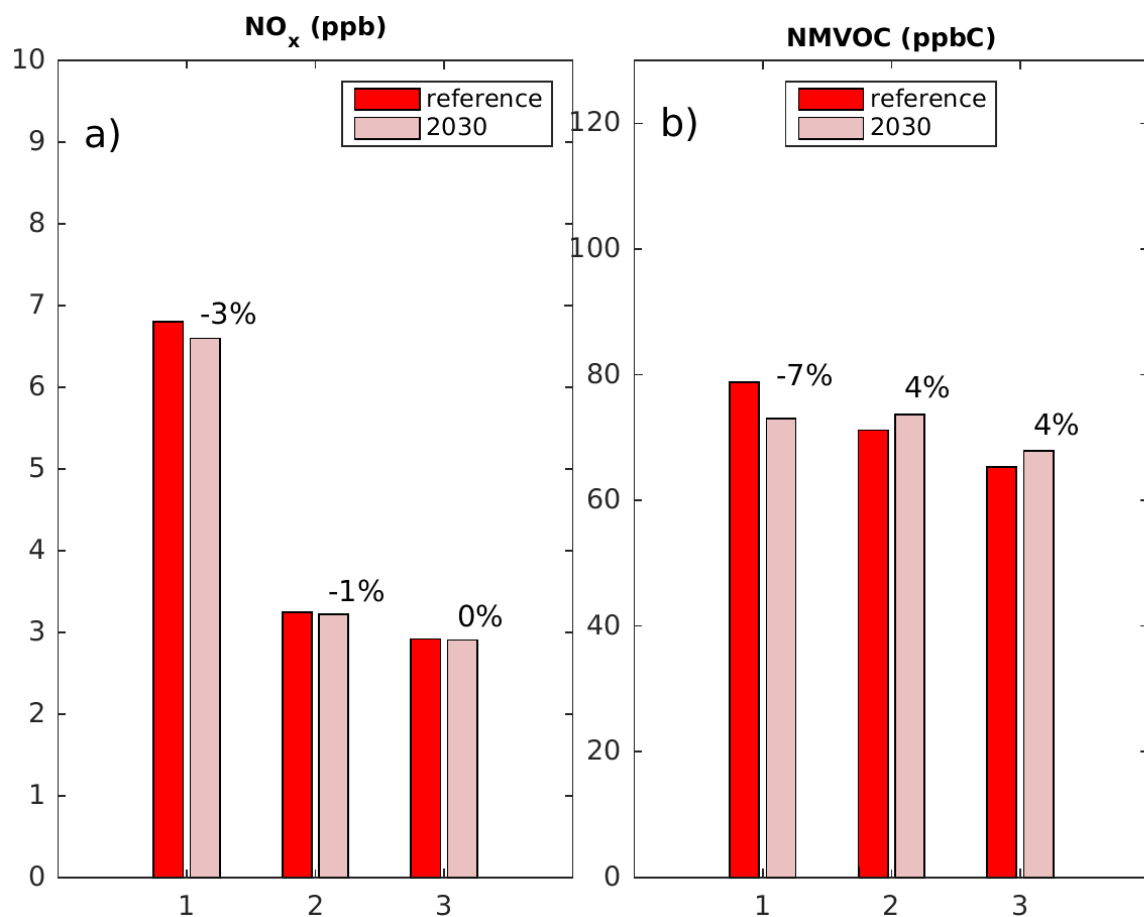


Figure S7. Surface mixing ratios of NO_x (a) and NMVOC (b) for the reference scenario (red) and the FC2030 scenario (pink) over the three selected regions during their corresponding season, highlighted in Fig.S6. The relative differences between both scenarios over each region are also indicated. The relative differences are calculated as: $([FC2030 - reference] / reference) \times 100\%$.

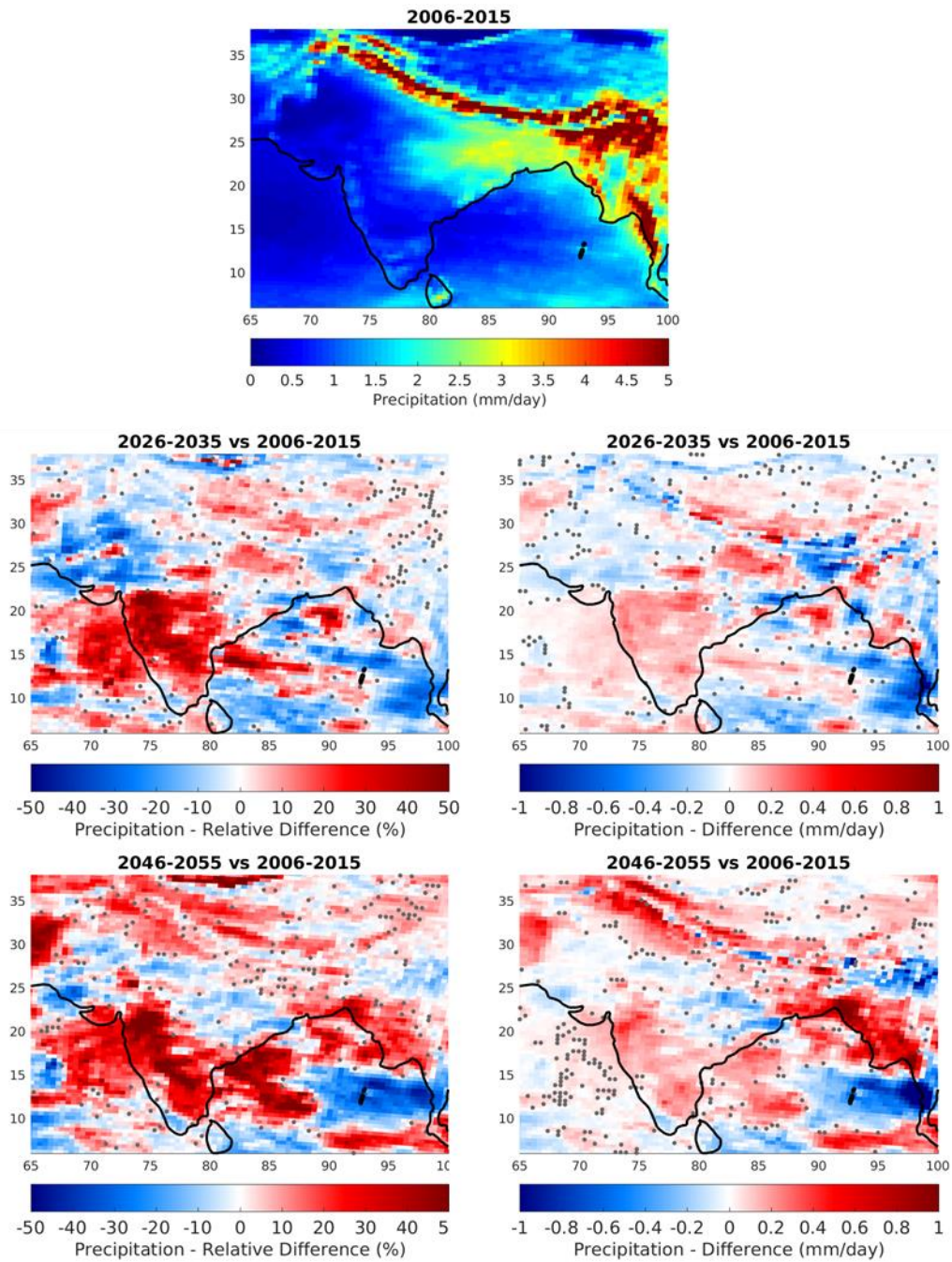


Figure S8. Distribution of precipitation (in mm/day) for the reference scenario (top panel), distribution of the relative difference and absolute difference in precipitation between the reference scenario and the FC2030 scenario (middle panels) and the FC2050 scenario (bottom panels). The relative differences are calculated as: $[(FC - \text{reference}) / \text{reference}] \times 100\%$, and the absolute differences as: $[FC - \text{reference}]$. Grey dots mark grid points that do not satisfy the 95% level of significance.

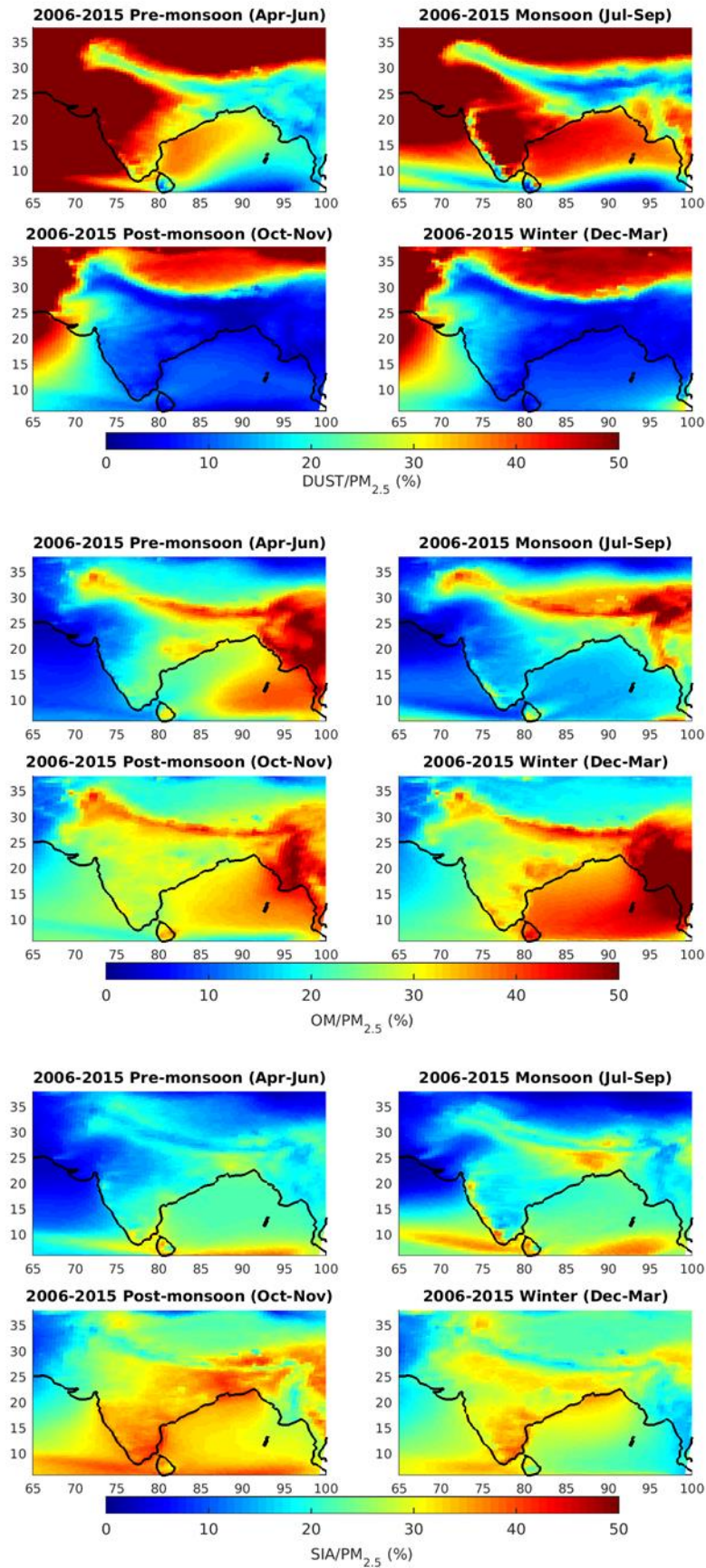


Figure S9. Seasonal distribution of ratio of dust (top panels), OM (mid-panels) and SIA (bottom panels) on surface $PM_{2.5}$ concentrations for the reference scenario.

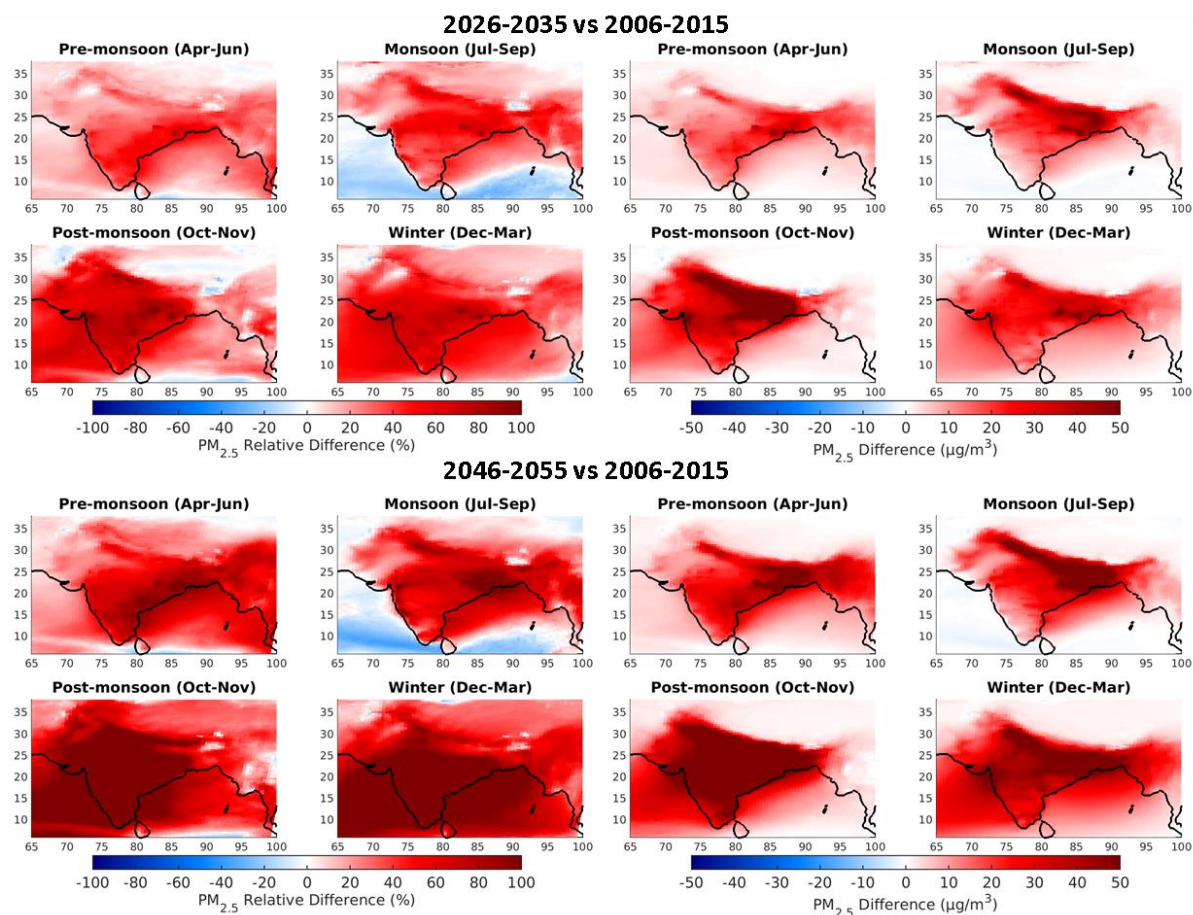


Figure S10. Seasonal distribution of the relative difference and absolute difference in surface PM_{2.5} between the reference scenario and the FCE2030 scenario (top panels) and the FCE2050 scenario (bottom panels). The relative differences are calculated as: $([FCE - reference] / reference) \times 100\%$, and the absolute differences as: $[FCE - reference]$.

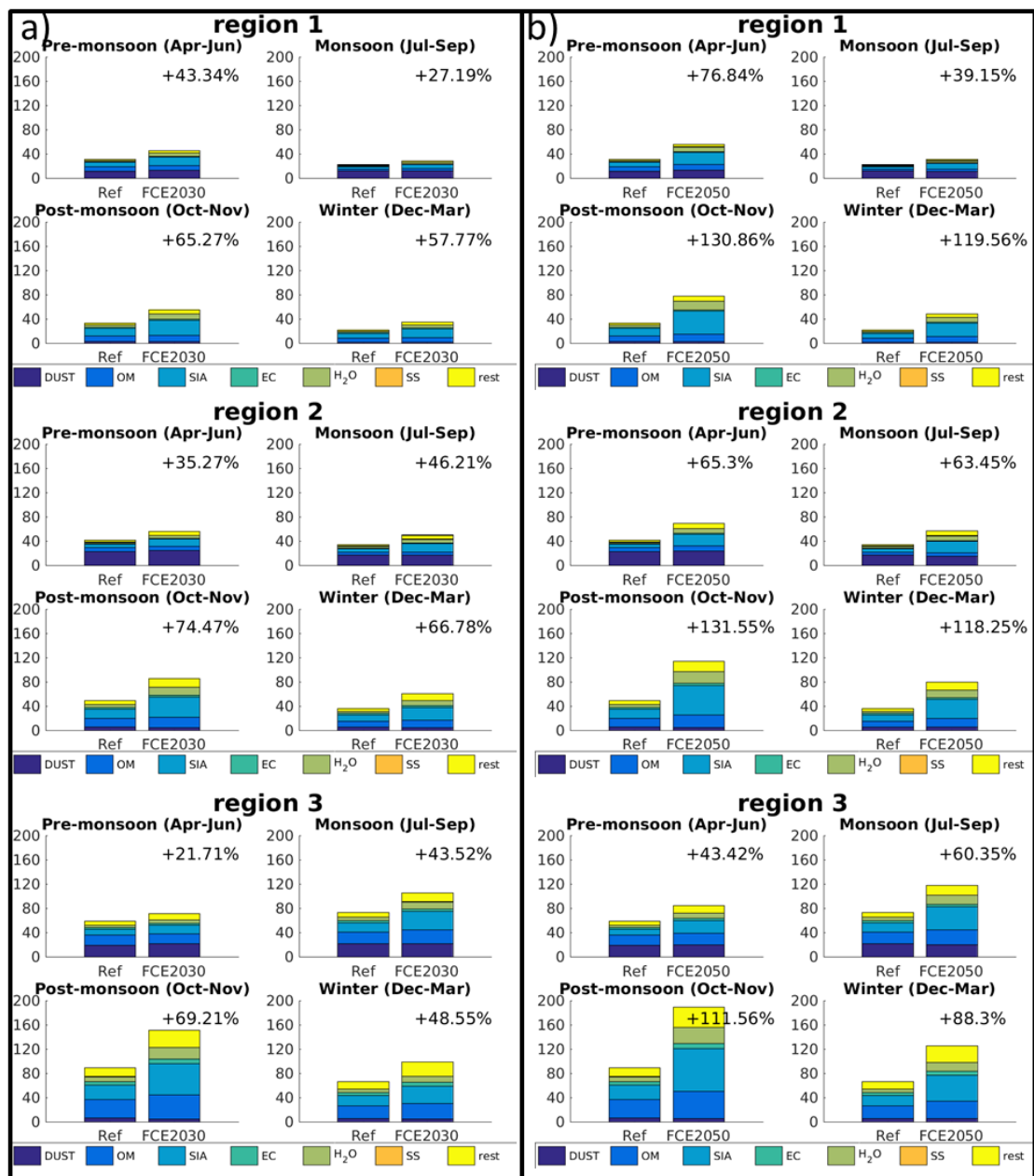


Figure S11. Seasonal composition of $PM_{2.5}$ (in $\mu g/m^3$) for the three regions highlighted by black boxes in Fig. 12 for the reference and the FCE2030 (a), and FCE2050 (b) scenarios. The black percent corresponds to the relative difference in $PM_{2.5}$ between the FCE scenarios and the reference scenario for each region.